Free Radical Biology and Medicine 75 (2014) 40–47

Contents lists available at ScienceDirect

Free Radical Biology and Medicine

journal homepage: www.elsevier.com/locate/freeradbiomed

Original Contribution

Monoamine oxidase inhibition prevents mitochondrial dysfunction and apoptosis in myoblasts from patients with collagen VI myopathies

E. Sorato [a,1], S. Menazza [a,2,1], A. Zulian [a], P. Sabatelli [b], F. Gualandi [c], L. Merlini [d], P. Bonaldo [e], M. Canton [a], P. Bernardi [a,f], F. Di Lisa [a,f,*]

[a] Department of Biomedical Sciences, University of Padova, 35131 Padova, Italy
[b] Institute of Molecular Genetics, National Research Council of Italy, 40136 Bologna, Italy
[c] Department of Medical Science, Section of Medical Genetics, University of Ferrara, 44100 Ferrara, Italy
[d] Laboratory of Musculoskeletal Cell Biology, Istituto Ortopedico Rizzoli, IRCCS, 40136 Bologna, Italy
[e] Department of Molecular Medicine, University of Padova, 35131 Padova, Italy
[f] Neuroscience Institute, National Research Council of Italy, 35131 Padova, Italy

ARTICLE INFO

Article history:
Received 20 February 2014
Received in revised form
24 June 2014
Accepted 3 July 2014
Available online 10 July 2014

Keywords:
Oxidative stress
Monoamine oxidases
Mitochondria
Muscular dystrophy
Cell death

ABSTRACT

Although mitochondrial dysfunction and oxidative stress have been proposed to play a crucial role in several types of muscular dystrophy (MD), whether a causal link between these two alterations exists remains an open question. We have documented that mitochondrial dysfunction through opening of the permeability transition pore plays a key role in myoblasts from patients as well as in mouse models of MD, and that oxidative stress caused by monoamine oxidases (MAO) is involved in myofiber damage. In the present study we have tested whether MAO-dependent oxidative stress is a causal determinant of mitochondrial dysfunction and apoptosis in myoblasts from patients affected by collagen VI myopathies. We find that upon incubation with hydrogen peroxide or the MAO substrate tyramine myoblasts from patients upregulate MAO-B expression and display a significant rise in reactive oxygen species (ROS) levels, with concomitant mitochondrial depolarization. MAO inhibition by pargyline significantly reduced both ROS accumulation and mitochondrial dysfunction, and normalized the increased incidence of apoptosis in myoblasts from patients. Thus, MAO-dependent oxidative stress is causally related to mitochondrial dysfunction and cell death in myoblasts from patients affected by collagen VI myopathies, and inhibition of MAO should be explored as a potential treatment for these diseases.

Introduction

Muscular dystrophies (MDs) are a group of inherited human diseases caused by mutations of genes encoding for different proteins of the extracellular matrix, the sarcoplasmic reticulum, or the cytoskeleton [1]. Typically, MDs are characterized by progressive skeletal muscle wasting and weakness [2].

The extracellular matrix protein collagen VI (ColVI) is a heterotrimeric protein involved in maintaining tissue integrity by providing a structural link between different constituents of connective tissue basement membranes and cells [3]. In humans, two major skeletal muscle diseases are caused by mutations in the genes coding for ColVI, namely Bethlem myopathy (BM) [4] and Ullrich congenital MD (UCMD) [5]. BM is relatively mild and in most cases slowly progressive, whereas UCMD is severe and shows diffuse wasting and weakness of skeletal muscles, associated with degeneration and regeneration of muscle fibers with a premature death due to respiratory failure [6].

Experimental models have allowed a better understanding of how the genetic defects result in loss of viability, and a crucial role has been attributed to mitochondrial dysfunction caused by opening of the mitochondrial permeability transition pore (PTP) [7–9]. However, the mechanisms linking mitochondrial derangements to defects in structural proteins interacting with the sarcolemma remain ill defined. A likely candidate is oxidative stress, since

Abbreviations: BM, Bethlem myopathy; ColVI, collagen VI; CsA, cyclosporine A; C_t, cycle threshold; Ctrl, controls; $\Delta\Psi_m$, mitochondrial membrane potential; FCCP, carbonyl cyanide *p*-trifluoromethoxyphenylhydrazone; GAPDH, glyceraldehyde-3-phosphate dehydrogenase; H_2O_2, hydrogen peroxide; MAO, monoamine oxidase; MD, muscular dystrophy; MTR, MitoTracker Red CM-H_2XRos; Parg, pargyline; PTP, permeability transition pore; R, rotenone; ROS, reactive oxygen species; TBS, Tris-buffered saline; TMRM, tetramethylrhodamine methyl ester; TUNEL, terminal deoxynucleotidyl transferase-mediated dUTP nick and labeling; Tyr, tyramine; UCMD, Ullrich congenital muscular dystrophy

* Corresponding author at: Department of Biomedical Sciences, University of Padova, Via Ugo Bassi, 58/B, 35131 Padova, Italy. Fax: +39 0498276140.
E-mail address: dilisa@bio.unipd.it (F. Di Lisa).

[1] These authors contributed equally to this work.

[2] Present address: Systems Biology Center, National Heart, Lung, and Blood Institute, National Institutes of Health, Bethesda, MD, USA.

http://dx.doi.org/10.1016/j.freeradbiomed.2014.07.006

increased levels of reactive oxygen species (ROS) have been documented as a causative effect in *mdx* mice, the murine model of Duchenne MD [10]. Oxidative stress may cause damage to proteins, membrane lipids, and DNA. Increased protein oxidation, as detected by carbonylation or thiol oxidation, was observed both in different experimental models of MDs [11,12] and in muscle biopsies from Duchenne MD patients [13]. Moreover, previous studies showed that antioxidant treatments were able to rescue MD phenotypes [14,15]. The most relevant ROS sources and their relationships with mitochondrial dysfunction remain unclear, however.

MAO are flavoproteins existing in two isoforms—MAO-A and MAO-B—that catalyze the oxidative deamination of neurotransmitters and dietary amines, generating aldehydes, ammonia, and hydrogen peroxide [16]. MAO catalyze catecholamine removal and have been widely studied in the central nervous system, while their impact in muscle function has been investigated only recently [11]. It must be considered that skeletal muscle is constantly exposed to the modulatory influence of neurohormones released by the sympathetic neurons and the adrenal gland. Many chronic diseases are characterized by an increased level of catecholamines, and this may include MD. For instance, in Duchenne patients the urinary catecholamine levels were found to be increased [17]. Of note, in a pioneer study a model of MD was obtained by serotonin administration associated with imipramine, an inhibitor of monoamine reuptake [18].

Increased expression of MAO occurs in many pathologies as well as in aging [19–21]. A number of transcription factors and hormones, such as corticosteroids, regulate in a different and complex way the two isoforms of the enzyme [22,23]. In *mdx* and ColVI null (*Col6a1*$^{-/-}$) mice we found an increase of the protein levels, as well as the enzymatic activity of MAO, suggesting that accumulation of ROS related to MAO activity plays a pivotal role in both loss of cell viability and contractile derangements [11]. Of note, we showed that treatment with pargyline, an inhibitor of both MAO-A and MAO-B [16], led to recovery from the dystrophic phenotype, indicating that in these diseases MAO are a major source of ROS and that their inhibition has a protective effect on muscle structure and function. Although MAO-induced ROS formation is likely to cause mitochondrial dysfunction, direct experimental evidence is still lacking.

This study aimed at assessing the role of MAO in the alterations of myoblasts obtained from patients with genetic defects of ColVI. The results show that treatment with the MAO inhibitor pargyline significantly reduced ROS accumulation and mitochondrial dysfunction while normalizing the occurrence of apoptosis. These findings prove a direct link between MAO-dependent oxidative stress and mitochondrial dysfunction caused by PTP opening.

Materials and methods

Participants

UCMD and BM were diagnosed according to the criteria of the European Neuromuscular Center [24]. All probands were examined and underwent a muscle biopsy. Genetic data for patients 1, 2, 4, and 5 have been published previously [5,25–28]. All participants provided written informed consent, and approval was obtained from the Ethics Committee of the Rizzoli Orthopedic Institute (Bologna, Italy). The basic features of the patients analyzed in this study are summarized in Table 1.

Myoblast cultures

Myoblast cultures were established from muscle biopsies of two healthy donors (Ctrl) and from UCMD (1–4) and BM (5) patients. Myoblasts were prepared by enzymatic and mechanical treatment of muscle biopsies, plated in DMEM supplemented with 20% FCS, penicillin, streptomycin, and amphotericin B as previously described [29], and stored in liquid nitrogen.

Immunoblotting

Western blot analysis was performed to evaluate MAO-B protein level. Briefly, myoblasts were seeded onto 75 cm^2 flasks, grown to confluence, and lysed in a buffer containing PBS, 1% NP-40, 1 mM NEM, 2 mM EDTA, protease (Complete mini EDTA-free, Roche Diagnostics, Indianapolis, IN), and phosphatase inhibitors (phosphatase inhibitor cocktail 3, Sigma). After centrifugation, the supernatant was collected and protein concentration was determined using Pierce BCA protein assay kit (Pierce, Rockford, IL). Equal amounts of protein (15 μg) were loaded onto 12% SDS-PAGE and electrophoretically transferred to nitrocellulose membrane (Bio-Rad Laboratories, Milan, Italy). Subsequently, after blocking in 5% fat-free dry milk in TBS (Tris-buffered saline) for 1 h at room temperature, samples were immunoblotted with the anti-monoamine oxidase B antibody M1821, and subsequently with horseradish peroxidase-conjugated secondary antibodies. Staining was detected by means of an enhanced chemiluminescence kit (LiteAblot Extend, EuroClone, Milan, Italy). Densitometric analysis was performed on the digital images obtained with Kodak Image station and software (Perkin Elmer, Boston, MA). The protein levels of MAO-B were quantified by image analysis using ImageJ software (National Institutes of Health, Bethesda, MD). MAO-B protein level was normalized to Red Ponceau staining as previously described [11].

Real time RT-PCR

To detect the MAO-A mRNA expression, myoblasts were seeded onto a 75 cm^2 flask and grown to confluence and total RNA was isolated with TRIzol Reagent (Life Technologies, Monza, Italy) and purified. Total RNA was then quantified with Nanodrop spectrophotometer (Thermo Scientific, Waltham, MA) and reverse-transcribed to the single-strand cDNA using the SuperScript III Reverse Transcriptase (Life Technologies). The Power SYBR Green PCR Master mix (Applied Biosystems, Foster City, CA) and the Rotor-Gene3000 detection system (Corbett Research, Cambridgeshire, UK) were used to estimate the mRNA of interest compared with the reference control. cDNA (1 μg) from the reverse transcription reactions was added to 20 μl reaction mixture for PCR. The PCR program included a denaturation step at 95 °C/9 min, 40 cycles of two amplification steps (95 °C/30 s and annealing extension at 58 °C/30 s), and melting curve (72–95 °C with a heating rate of 1 °C/5 s). The following primers were used for MAO-A (GenBank Accession Number NM_000240): forward primer, 5′-AGCGGCTACATGGAAGGGGCA-3′; and reverse primer, 5′-AGGCCAGAAACAGAGGGCAGGTT-3′; amplicon size, 179 bp. All samples were amplified in triplicate and the human glyceraldehyde-3-phosphate dehydrogenase (GAPDH) was used as the reference gene to normalize the data (GenBank Accession Number NM_002046): forward primer 5′-ACGGATTTGGTCGTATTGGG-3′; and reverse primer, 5′-CTCCTGGAAGATGGTGATGG-3′; amplicon size, 212 bp. The specificity of the amplification was tested at the end of each run by melting curve analysis, using the Rotor-Gene software.

During the exponential phase, the fluorescence signal threshold was calculated and the number of PCR cycles required to reach the threshold (cycle threshold, C_t) was determined. C_t values decreased linearly with increasing input target quantity and were used to calculate the relative mRNA expression, according to the mathematical quantification model proposed by Pfaffl, which

Table 1
Clinical and genetic features of patients included in the study.

Patient	Phenotype	Clinical features	Mutation(s)	Collagen VI	Refs.
P1	UCMD	Floppy at birth, walker 3–7 yrs, DL, FC, SC, MV age 10 yrs.	COL6A2 heterozygous intron 17 c.1459-2 A > G; p.Gly 487-Ala495delAspfsX48 and Heterozygous intron 23 c.1771-1G > A; p.Glu591-Cys605delThrfsX148	Marked reduction	[5,25]
P2	UCMD	Floppy at birth, CHD, DL, FC, SC, walker 20 ms-6 yrs, MV age 11 yrs.	COL6A1 heterozygous exon 8 c.798_804+8del 15; p.Pro254_Glu268del	Reduced at the basal lamina	[28]
P3	UCMD	Floppy at birth, CHD, FC, DL, SC, aided walker age 5 yrs.	COL6A2 homozygous exon 28 c.2572 C > T omo; p.Gln858X*	Reduced at the basal lamina	
P4	UCMD	Floppy at birth, NAW, DL, FC, SC, RI age 10 yrs.	COL6A1 heterozygous exon 9 c. 819_833del; p.Pro274_Gly278del	Reduced at the basal lamina	[27]
P5	BM	Early onset, never able to run, diffuse contractures, W age 30, moderate RI.	COL6A2 heterozygous exon 26 c.2098 G > A; p.Gly700Ser	Normal	[26]

ColVI levels are based on immunohistochemistry as described in the original references, which also contain further details about the gene mutations and their mode of inheritance. DL, distal laxity; FC, finger contractures; SC, skin changes (keloid formation, follicular hyperkeratosis); MV, nocturnal mechanical ventilation; W, walker; NAW, never able to walk; RI, respiratory insufficiency; CHD, congenital hip dislocation.

defines a parameter for the relative gene expression [30]. This parameter is significantly higher or lower than 1.0 when up-regulation or down-regulation of the gene of interest occurs, respectively [31].

ROS detection

Mitochondrial ROS was detected using the fluorescent probe MitoTracker Red CM-H_2XRos (MTR, Molecular Probes, Eugene, OR). Myoblasts were seeded onto 24-mm-diameter round glass coverslips and grown for 2 days in DMEM supplemented with 20% FCS. Cells were rinsed once and then incubated with the MAO inhibitor pargyline (100 μM) for 20 min in serum-free DMEM, followed by H_2O_2 (100 μM) or tyramine (20 μM) for 45 min. Finally, myoblasts were loaded with MTR (20 nM) for 15 min. All the steps were carried out at 37 °C with 5% CO_2. Myoblasts were then washed twice and the chambered coverslips transferred to an Olympus IMT-2 inverted microscope (Center Valley, PA), equipped with a xenon lamp and a 12-bit digital cooled CCD camera (Micromax, Princeton Instruments, Trenton, NJ). Mitochondrial fluorescence was measured in 10–15 random fields per chamber and data were averaged per field. For each group, 4–6 chambers were generally analyzed. Experiments with the different agents as described above were always performed in comparison with their respective controls. Fluorescence emission was monitored by using 568 ± 25 nm excitation and 585 nm longpass emission filter setting. Images were collected with an exposure time of 100 ms by using a x40, 1.3 N.A. oil immersion objective. Data were acquired and analyzed using Metafluor software (Universal Imaging).

Mitochondrial membrane potential

This parameter was measured based on the accumulation of tetramethylrhodamine methyl ester (TMRM, Molecular Probes). The extent of cell and, hence, mitochondrial loading with potentiometric probes is affected by the activity of the plasma membrane multidrug resistance pump. To prevent probe release through this system, in all experiments with TMRM the medium was supplemented with 1.6 μM CsH, which inhibits the multidrug resistance pump but not the PTP [32]. Myoblasts were treated with tyramine (20 μM) for 30 min in the absence or in the presence (as a 20 min pretreatment) of MAO inhibitor pargyline (100 μM) or CsA (1.6 μM), followed by the addition of 25 nM TMRM. At the end of each experiment, mitochondria were fully depolarized by the addition of the protonophore carbonyl cyanide *p*-trifluoromethoxyphenylhydrazone (FCCP, 4 μM). Images were collected and analyzed as detailed in the previous section. TMRM fluorescence was evaluated as the difference between values obtained before and after FCCP.

Rotenone (2 μM) was added after treatment for 40 min with pargyline (100 μM). Clusters of several mitochondria (10–30) were identified as regions of interest, and fields not containing cells were taken as the background. Sequential digital images were acquired every 2 min, and the average fluorescence intensity of all relevant regions was recorded and stored for subsequent analysis.

Detection of apoptosis

The rate of apoptosis was measured in myoblast cultures using the terminal deoxynucleotidyltransferase-mediated dUTP nick end labeling (TUNEL) method. Myoblast cultures were seeded onto 12-mm-diameter round glass coverslips and grown to confluence in DMEM supplemented with 20% FCS. Cells were then incubated in serum-free DMEM in the presence or in absence of MAO inhibitor pargyline (100 μM) and staurosporine (1 μM) as positive control for 24 h. Cells were fixed in 50% acetone/50% methanol and processed for TUNEL analysis by using the DeadEnd Fluorometric TUNEL System (Promega, Madison, WI). Visualization of all nuclei was performed by staining with Hoechst 33258. The number of total and TUNEL-positive nuclei was determined in randomly selected fields by using a Zeiss (Oberkochen, Germany) Axioplan microscope (× 40 magnification) equipped with a digital camera.

Data analysis and statistical procedures

All data are expressed as the mean ± SEM. Comparisons between two groups were performed using nonpaired two-sample Student's *t* test, and values with $P < 0.05$ were considered significant.

Chemicals

Unless otherwise stated all chemicals used were purchased from Sigma-Aldrich (St. Louis, MO, USA).

Results

The increased ROS level in myoblasts from patients affected by ColVI myopathies is reduced by MAO inhibition

We studied myoblasts from four UCMD patients and one BM patient (Table 1). The patients affected by UCMD have different mutations, located either in the triple helical domain or in the C-terminal region of different ColVI chains. Patients 1 and 3 were recessive UCMD cases, whereas patients 2 and 4 carried dominant *de novo* mutations. The mutation detected in patient 3, a nonsense change located in the last *COL6A2* exon, has never been reported before.

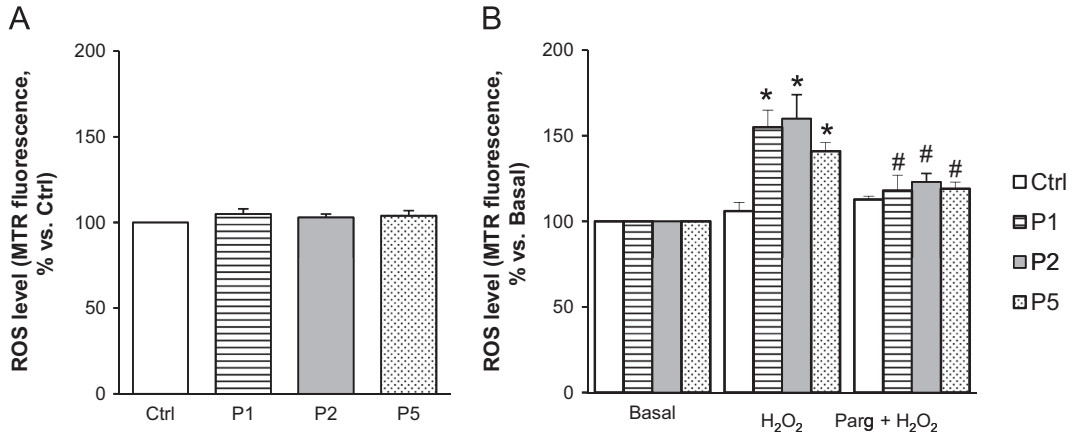

Fig. 1. MAO inhibition decreases ROS accumulation in response to oxidative stress in myoblasts from patients affected by ColVI myopathies. (A) Myoblasts from UCMD (P1 and P2), BM (P5) patients, and healthy donors (Ctrl) were loaded with Mitotracker Red CM-H_2XRos (MTR, 25 nM). Data are reported as the MTR fluorescence after 15 min. (B) Myoblasts from UCMD (P1 and P2), BM (P5) patients, and healthy donors (Ctrl) were loaded with Mitotracker Red CM-H_2XRos (MTR, 25 nM). Oxidative stress was induced by H_2O_2 addition (100 μM) in the absence or in the presence of pargyline (100 μM, as a 20 min pretreatment), namely H_2O_2 or Parg + H_2O_2 respectively. Data expressed as the MTR fluorescence after 40 min from the addition of H_2O_2 were normalized to the values obtained in the absence of H_2O_2 (Basal) for each samples. Values are the mean of at least four independent experiments. $^*P < 0.05$ for H_2O_2–treated vs Basal; $\#P < 0.05$ for Parg + H_2O_2-treated vs H_2O_2-treated myoblasts.

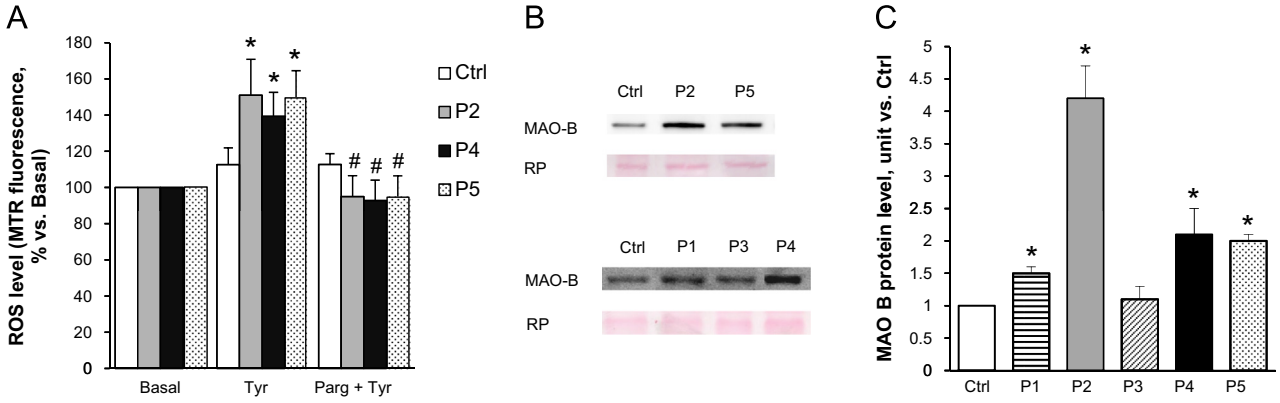

Fig. 2. MAO inhibition prevents tyramine-induced increase in ROS level in myoblasts from patients affected by ColVI myopathies. (A) Myoblasts from UCMD (P2 and P4), BM (P5) patients, and healthy donors (Ctrl) were incubated with the substrate for both MAO-A and MAO-B tyramine (20 μM), in the absence or in the presence of the MAO inhibitor pargyline (100 μM, as a 20 min pretreatment), namely Tyr or Parg + Tyr, respectively. ROS accumulation was assessed by Mitotracker Red CM-H_2XRos (MTR, 25 nM). Data expressed as the MTR fluorescence after 1 h from the addition of tyramine were normalized to the values obtained in the absence of tyramine (Basal) for each samples. Values are the mean of at least four independent experiments. $^*P < 0.05$ for Tyr-treated vs Basal; $\#P < 0.05$ for Parg + Tyr-treated vs Tyr-treated myoblasts. (B) MAO-B protein level was detected by Western blotting in myoblasts from UCMD (P1-P4), BM (P5) patients, and healthy donors (Ctrl). (C) The bands were quantitated by densitometry and data are expressed as the ratio of MAO-B to Red Ponceau staining. Data shown in the panel are the mean of at least four experiments. $^*P < 0.05$ for each patient vs healthy donor.

First, we investigated the susceptibility to oxidative stress. Under basal conditions (i.e., in the absence of stimuli promoting ROS formation) ROS levels did not show major differences between myoblasts from healthy donors and patients (Fig. 1A). However, when myoblasts were incubated with hydrogen peroxide (100 μM), the level of ROS was significantly higher in patients affected by UCMD and BM than in myoblasts from healthy donors (Fig. 1B). Interestingly, the MAO inhibitor pargyline was able to abolish the accumulation of ROS, suggesting that MAO play a role in the response of cells from patients to oxidative stress.

To investigate more directly the role of MAO, we next incubated myoblasts with tyramine, a substrate for both MAO-A and MAO-B. A higher level of ROS was detected in patient myoblasts as compared with healthy donor cells and, importantly, this abnormal ROS increase was prevented by pargyline (Fig. 2A). The pargyline-inhibitable ROS accumulation was associated with an increase in MAO-B protein levels in patient myoblasts (Fig. 2B and C). Unfortunately, the available anti-MAO-A antibodies do not recognize reliably this isoform in patient myoblasts. A similar problem exists for mRNA expression of both MAO-A and MAO-B that was barely detectable according to previous reports [33]. Notably, however, we could measure an increase in MAO-A mRNA expression (1.80 ± 0.19, $P=0.011$, and 1.35 ± 0.27, $P=0.163$, for patient 2 and 5, respectively) only in the two patients displaying high MAO activity.

MAO activity contributes to mitochondrial dysfunction in myoblasts from patients affected by ColVI myopathies

Previous results demonstrated occurrence of mitochondrial dysfunction in fibers from skeletal muscle of *Col6a1*$^{-/-}$ mice [7], as well as in myoblasts from patients affected by UCMD [27,34]. The role of the intracellular MAO-dependent ROS accumulation on mitochondrial function in muscle cell cultures was investigated by assessing mitochondrial membrane potential ($\Delta\Psi_m$) with TMRM. To exclude artifacts due to the different loading capacity of the various cells, which can be erroneously interpreted as $\Delta\Psi_m$ differences, FCCP, an uncoupler that collapses $\Delta\Psi_m$, was added at

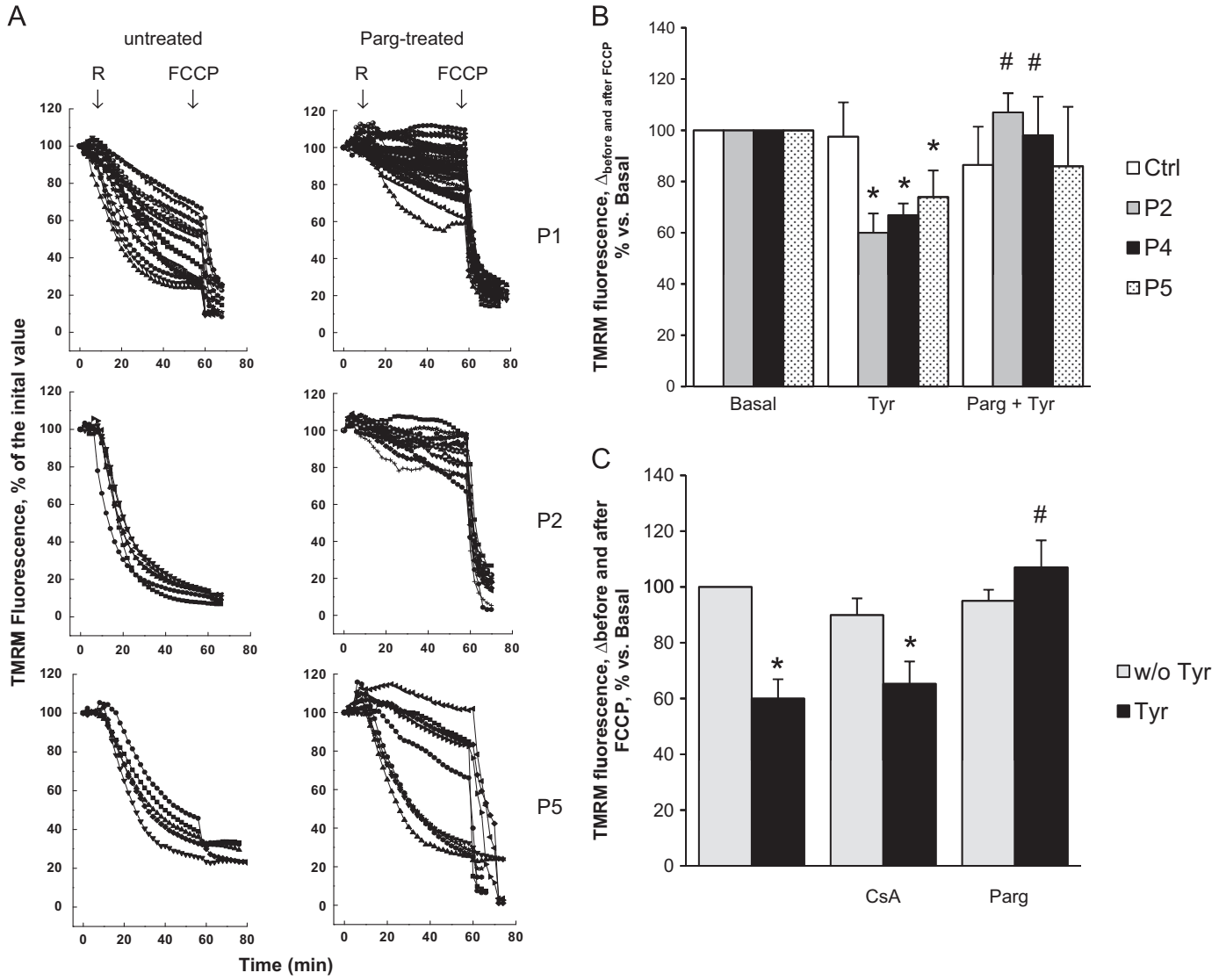

Fig. 3. MAO inhibition prevents mitochondrial dysfunction in myoblasts from patients affected by ColVI myopathies. (A) Rotenone-induced mitochondrial dysfunction. The upper, middle, and lower traces refer to the UCMD patients P1 and P2, and the BM patient B5, respectively. Myoblasts were loaded with TMRM (25 nM) to monitor the mitochondrial membrane potential by fluorescence microscopy. When indicated by arrows, rotenone (R, 2 μM) and FCCP (4 μM) were added (all traces) in the absence of further treatments (untreated) or after treatment for 40 min with pargyline (Parg-treated, 100 μM). Each trace corresponds to one cell. (B) Tyramine-induced mitochondrial dysfunction. Myoblasts from UCMD (P2 and P4), BM (P5) patients, and healthy donors (Ctrl) were incubated as described in Fig. 2A and then loaded with TMRM (25 nM). At the end of each experiment the uncoupling agent FCCP (4 μM) was added. The difference of fluorescence intensities obtained before and after FCCP is reported in the graph. Values are the mean of at least four independent experiments. $^{*}P < 0.05$ for Tyr-treated vs Basal; $\#P < 0.05$ for Parg + Tyr-treated vs Tyr-treated myoblasts. (C) CsA does not prevent mitochondrial dysfunction induced by tyramine. Myoblasts from a UCMD patient (P2) were incubated for 1 h with tyramine (Tyr, 20 μM, black bars) in the absence or in the presence of CsA (1.6 μM, as a 20 min pretreatment) or pargyline (Parg, 100 μM, as a 20 min pretreatment) and then loaded with TMRM (25 nM) to assess the mitochondrial membrane potential as described in panel B. All the treatments were also performed in the absence of tyramine (w/o Tyr, gray bars). Values are the mean of at least four independent experiments. $^{*}P < 0.05$ for Tyr-treated vs Tyr-untreated myoblasts; $\#P < 0.05$ for Parg + Tyr-treated vs Tyr-treated myoblasts.

the end of each experiment. Thus, in each cell the difference of fluorescence intensities obtained before and after FCCP provides a reliable assessment of $\Delta\Psi_m$ [35].

In keeping with our previous results [36], addition of the complex I inhibitor rotenone to patient cells promptly caused mitochondrial depolarization (Fig. 3A), in contrast to cultures from healthy donors in which mitochondrial membrane potential is maintained by ATP hydrolysis due to the inverted operation of F_OF_1 ATP synthase. Interestingly, the response to rotenone was completely normalized by treatment with the MAO inhibitor pargyline, suggesting that the latent mitochondrial dysfunction in myoblasts from UCMD and BM patients can be amplified selectively by MAO-dependent ROS production (Fig. 3A).

To further investigate the role of MAO, myoblasts were incubated with the MAO substrate tyramine (Fig. 3B). It is worth noting that myoblasts cannot be exposed to continuous light in the presence of tyramine, probably due to the combined formation of ROS by tyramine and photosensitization by TMRM. $\Delta\Psi_m$ was therefore measured as an endpoint after 1 h of incubation. Tyramine addition to cultures caused a drop in $\Delta\Psi_m$ only in cells from UCMD and BM patients. Remarkably, the decrease in mitochondrial membrane potential was fully prevented by treatment with pargyline, suggesting that reduced production of ROS due to MAO activity was paralleled by improved mitochondrial function (Fig. 3B). Although a role of oxidative stress in pathogenesis of MD has been suggested in several reports, the present findings assign a central role to MAO as the source, and to mitochondria as the target, in causing dysfunction and cell death of dystrophic myocytes.

CsA prevents mitochondrial dysfunction in myoblasts from UCMD patients by desensitizing the PTP [27]. We tested whether

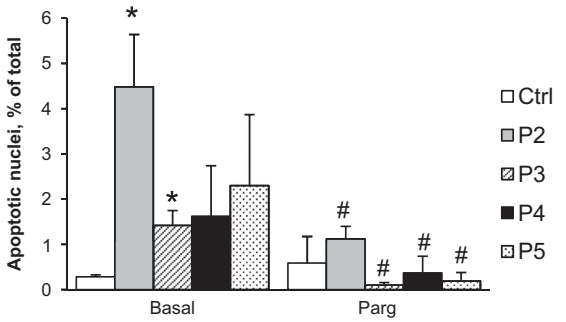

Fig. 4. MAO inhibition decreases apoptosis in myoblasts from patients affected by ColVI myopathies. Primary myoblast cultures from a healthy donor (Ctrl), UCMD (P2–P4), and BM (P5) patients were scored for the presence of TUNEL-positive nuclei after 24 h incubation in the absence (Basal) or in the presence of pargyline (Parg, 100 μM). Data are the mean of three independent experiments ± SEM. $^{*}P < 0.05$ for each patient vs healthy donor; #, not significant for each patient vs healthy donor.

CsA reduces mitochondrial dysfunction due to MAO-dependent ROS accumulation as well. Unlike pargyline, CsA could not prevent mitochondrial depolarization induced by tyramine (Fig. 3C). These data suggest that MAO-dependent ROS accumulation is upstream of PTP opening, and that oxidative stress makes the latter event insensitive to CsA.

The incidence of apoptosis in myoblasts from patients affected by ColVI myopathies is reduced by MAO inhibition

The occurrence of apoptosis was evaluated in myoblasts from UCMD and BM patients. As already demonstrated by Angelin et al. [27], cells from dystrophic patients displayed a higher incidence of apoptosis compared to cells from healthy donors. Here, we found that the MAO inhibitor pargyline reduced the occurrence of apoptosis to baseline levels (Fig. 4).

A mild cellular phenotype requires stronger stimuli to elicit mitochondrial dysfunction.

Fig. 5B shows that tyramine induced a less severe mitochondrial depolarization in patient 3 compared to other patients (Fig. 3B). In addition, the concentration needed to induce this effect was 5-fold higher (100 μM) and the effect of rotenone was reduced (Fig. 5C). Notably, this milder cellular phenotype was associated with the lowest amount of MAO-B protein level (Fig. 2B) and extent of apoptosis (Fig. 4), supporting the relevance of MAO-induced oxidative stress in mitochondrial dysfunction and cell death in dystrophic myocytes. A similar association among MAO expression, oxidative stress, and negative outcome has been recently described for human atrial fibrillation [37].

Discussion

The present findings demonstrate a relevant role for MAO-dependent ROS production in human ColVI myopathies. Indeed, (i) oxidative stress is strongly linked to cell death in MDs; (ii) a causal relationship exists between MAO-dependent ROS formation and mitochondrial dysfunction; (iii) MAO activity plays a determinant role in these pathologies; and (iv) MAO inhibition is able to prevent the ROS accumulation, mitochondrial dysfunction, and loss of cell viability that characterize these pathologies.

MAO and mitochondrial dysfunction in MDs

We previously demonstrated in MD murine models that MAO-dependent oxidative stress is causally linked to both contractile dysfunction and cell death [11]. MAO involvement in MDs has been already suggested by studies carried out during the seventies, when the genetic causes of MD pathologies were still unknown. In particular, catecholamines and their metabolites were shown to be increased in experimental and clinical MDs [17,38,39]. Moreover, the alteration in catecholamine metabolism was shown to correlate with disease severity [17], in keeping with the present observation that in patient 3 a lower MAO expression and activity are associated with a less severe cellular phenotype.

The present results also demonstrate that oxidative stress generated by increased MAO activity causes mitochondrial dysfunction, matching evidence obtained in neonatal cardiac myocytes [40]. Therefore, the larger ROS formation due to an increased MAO activity contributes to bridge the gap between alterations of ColVI and mitochondrial derangements responsible for the functional and structural abnormalities of MDs [7,27].

Although mitochondrial dysfunction is commonly associated with increased ROS levels, the precise mechanisms through which oxidative stress causes mitochondrial dysfunction have not been elucidated conclusively. ROS could modulate the expression level and posttranslational modification of proteins involved in mitochondrial dysfunction. For instance, Cys 39 nitrosylation in ND3 subunit of mitochondrial complex I has been associated with myocardial protection against ischemia/reperfusion injury [41]. Cyclophilin D (CypD) oxidation at Cys 203 appears to be necessary for PTP opening related to oxidative stress [42]. An additional relevant target of ROS is F_OF_1 ATP synthase. Multiple posttranslational oxidative modifications occur at Cys 294 in the α-subunit, providing evidence for the role of this residue as a redox sensor [43]. In addition, posttranslational modifications (namely disulfide bonds between Cys 294 neighboring α-subunits) cause F_OF_1 ATP synthase inhibition in a model of heart failure [43]. Besides modifications in complex I and CypD, ROS-induced changes in F_OF_1 ATP synthase are likely to be relevant for promoting PTP opening. Indeed, the molecular identity of the PTP has been attributed recently to the dimerization of F_OF_1 ATP synthase [44]. Based on the present findings, MAO-dependent ROS formation is likely to contribute to mitochondrial protein oxidative modifications that result in PTP opening and mitochondrial dysfunction.

The role of PTP in MD is supported by numerous studies showing that pharmacological inhibition or genetic ablation of CypD ameliorates biochemical and structural alterations in different models of MD [7–9]. It is worth noting that CypD is not a PTP component but just one of its many modulators. Therefore, a lack of effect of CypD inhibition is far from being a convincing argument to rule out the involvement of PTP opening in a given condition. This concept, which unfortunately is frequently overlooked, applies also to the present findings that CsA does not prevent the collapse of $\Delta\Psi_m$ when MAO activity is maximal due to tyramine addition. It is tempting to speculate that severe oxidative stress reduces the voltage threshold for PTP opening [36], making this process independent of CypD inhibition. Accordingly, an excessive ROS formation would mimic a condition of intramitochondrial Ca^{2+} overload where PTP opening is observed also in the presence of CypD inhibition or deletion [45,46]. This hypothesis might also contribute to explain why treatment of MD patients with CsA displayed partial efficacy, with correction of mitochondrial alterations and reduced cell death in the limbs, but not in respiratory muscles [47].

Treatment of secondary pathological changes has enormous potential to improve the quality of life and to extend life span in MD patients. Although many studies have reported that MDs are

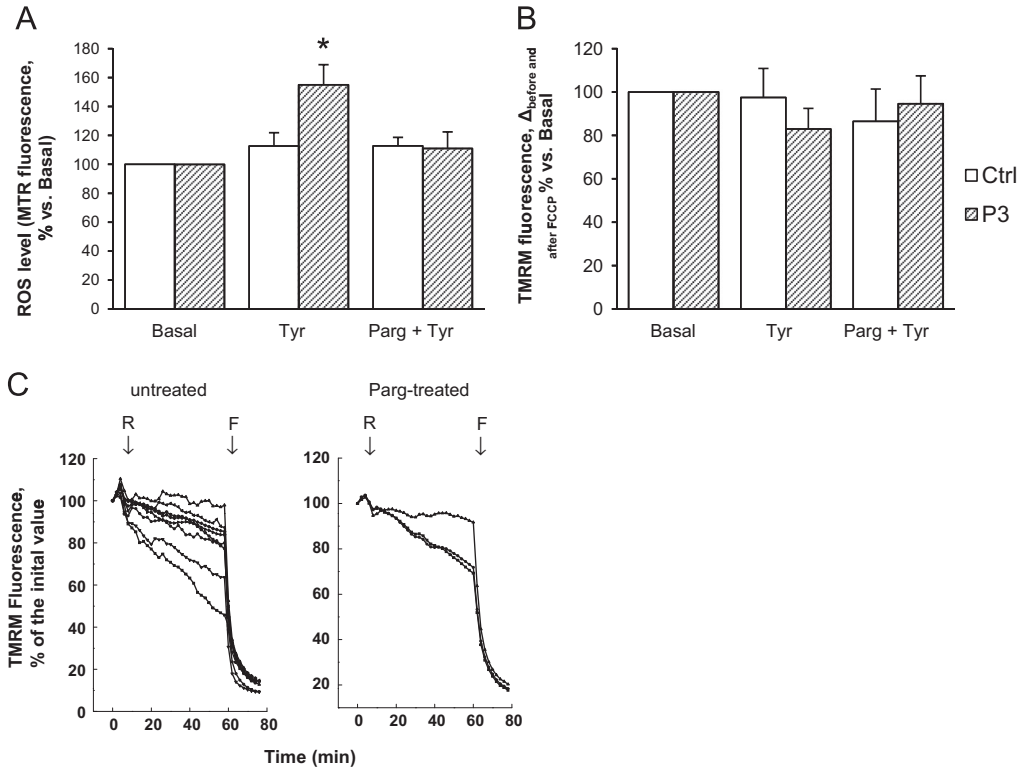

Fig. 5. Mitochondrial dysfunction in a milder UCMD myoblast phenotype requires stronger stimuli. (A) Myoblasts from a UCMD patient (P3) and healthy donors (Ctrl) were incubated for 1 h with tyramine (100 μM) in the absence or in the presence of pargyline (100 μM, as a 20 min pretreatment), namely Tyr or Parg + Tyr, respectively. Myoblasts were incubated also in the absence of tyramine (Basal). ROS accumulation was assessed by Mitotracker Red CM-H_2XRos (MTR, 25 nM) as described in Fig. 2A. Values are the mean of at least four independent experiments. $^*P < 0.05$ for Tyr-treated vs Basal. (B) Myoblasts from the UCMD (P3) patient and healthy donors (Ctrl) were incubated as described in (A) and then loaded with TMRM (25 nM) to assess the mitochondrial membrane potential as described in Fig. 3. Values are the mean of at least four independent experiments. (C) Myoblasts from UCMD patient (P3) were loaded with TMRM (25 nM). When indicated by arrows, rotenone (R, 2 μM) and FCCP (4 μM) were added (all traces) in the absence of further treatments (untreated) or after treatment for 40 min with pargyline (Parg-treated, 100 μM). Each trace corresponds to one cell.

associated with oxidative stress in both animal models and in patients [13,48], the sources of ROS and their involvement remained ill defined. Obviously, this is a prominent concern for developing antioxidant interventions [49]. Several antioxidants, such as *N*-acetylcysteine or polyphenols from green tea extracts, demonstrated their efficacy in ameliorating the muscle pathophysiology of a Duchenne mouse model [14,15], but these drugs can only reduce the levels of ROS that are already formed, by acting as scavengers. MAO inhibitors instead act by preventing ROS formation, thus making this class of drugs more attractive.

Study limitations

As reported previously [50], myoblasts after 9 passages lose their mitochondrial phenotype. To reduce variability due to this limitation we performed experiments until the 8th passage. Moreover, besides the scarce reliability of MAO-A antibodies and low level of expression of its mRNA described above, an additional limitation of the study is the lack of functional characterization that cannot be carried out in myoblasts.

Conclusions

The present findings extend to myoblasts from UCMD and BM patients previous results obtained in murine models of MD, demonstrating that: (i) increased MAO expression and activity cause an increase in ROS level, and (ii) MAO-dependent ROS production induces mitochondrial dysfunction involved in cell death. These results provide a rationale for future clinical trials with MAO inhibitors, well-characterized drugs already used for the treatment of neurological disorders.

Acknowledgments

We gratefully acknowledge Prof. Ellen Billett and Dr. Asli Ugun Klusek for analysis of MAO A expression and constructive comments. This work was supported by grants from the University of Padova (Fondazione Cariparo to F.D.L.); the Italian Ministry for University and Research (PRIN to M.C.); National Research Council of Italy (to F.D.L.); French Muscular Dystrophy Association (to M.C.); and Telethon Foundation (Grant GGP11082). The authors declare that they have no conflict of interests.

References

[1] Shin, J.; Tajrishi, M. M.; Ogura, Y.; Kumar, A. Wasting mechanisms in muscular dystrophy. *Int. J. Biochem. Cell Biol.* **45:**2266–2279; 2013.
[2] Cohn, R. D.; Campbell, K. P. Molecular basis of muscular dystrophies. *Muscle Nerve* **23:**1456–1471; 2000.
[3] Keene, D. R.; Engvall, E.; Glanville, R. W. Ultrastructure of type VI collagen in human skin and cartilage suggests an anchoring function for this filamentous network. *J. Cell Biol.* **107:**1995–2006; 1988.
[4] Bethlem, J.; Wijngaarden, G. K. Benign myopathy, with autosomal dominant inheritance. A report on three pedigrees. *Brain* **99:**91–100; 1976.
[5] Camacho Vanegas, O.; Bertini, E.; Zhang, R. Z.; Petrini, S.; Minosse, C.; Sabatelli, P.; Giusti, B.; Chu, M. L.; Pepe, G. Ullrich scleroatonic muscular dystrophy is caused by recessive mutations in collagen type VI. *Proc. Natl. Acad. Sci. USA* **98:**7516–7521; 2001.
[6] Allamand, V.; Brinas, L.; Richard, P.; Stojkovic, T.; Quijano-Roy, S.; Bonne, G. ColVI myopathies: where do we stand, where do we go? *Skelet. Muscle* **1:**30; 2011.
[7] Irwin, W. A.; Bergamin, N.; Sabatelli, P.; Reggiani, C.; Megighian, A.; Merlini, L.; Braghetta, P.; Columbaro, M.; Volpin, D.; Bressan, G. M.; Bernardi, P.; Bonaldo, P.

Mitochondrial dysfunction and apoptosis in myopathic mice with collagen VI deficiency. *Nat. Genet.* **35:**367–371; 2003.
[8] Millay, D. P.; Sargent, M. A.; Osinska, H.; Baines, C. P.; Barton, E. R.; Vuagniaux, G.; Sweeney, H. L.; Robbins, J.; Molkentin, J. D. Genetic and pharmacologic inhibition of mitochondrial-dependent necrosis attenuates muscular dystrophy. *Nat. Med.* **14:**442–447; 2008.
[9] Palma, E.; Tiepolo, T.; Angelin, A.; Sabatelli, P.; Maraldi, N. M.; Basso, E.; Forte, M. A.; Bernardi, P.; Bonaldo, P. Genetic ablation of cyclophilin D rescues mitochondrial defects and prevents muscle apoptosis in collagen VI myopathic mice. *Hum. Mol. Genet.* **18:**2024–2031; 2009.
[10] Rando, T. A. Oxidative stress and the pathogenesis of muscular dystrophies. *Am. J. Phys. Med. Rehabil.* **81:**S175–S186; 2002.
[11] Menazza, S.; Blaauw, B.; Tiepolo, T.; Toniolo, L.; Braghetta, P.; Spolaore, B.; Reggiani, C.; Di Lisa, F.; Bonaldo, P.; Canton, M. Oxidative stress by monoamine oxidases is causally involved in myofiber damage in muscular dystrophy. *Hum. Mol. Genet.* **19:**4207–4215; 2010.
[12] Terrill, J. R.; Radley-Crabb, H. G.; Iwasaki, T.; Lemckert, F. A.; Arthur, P. G.; Grounds, M. D. Oxidative stress and pathology in muscular dystrophies: focus on protein thiol oxidation and dysferlinopathies. *FEBS J.* **280:**4149–4164; 2013.
[13] Haycock, J. W.; MacNeil, S.; Jones, P.; Harris, J. B.; Mantle, D. Oxidative damage to muscle protein in Duchenne muscular dystrophy. *Neuroreport* **8:**357–361; 1996.
[14] Dorchies, O. M.; Wagner, S.; Vuadens, O.; Waldhauser, K.; Buetler, T. M.; Kucera, P.; Ruegg, U. T. Green tea extract and its major polyphenol (-)-epigallocatechin gallate improve muscle function in a mouse model for Duchenne muscular dystrophy. *Am. J. Physiol. Cell Physiol.* **290:**C616–C625; 2006.
[15] Whitehead, N. P.; Pham, C.; Gervasio, O. L.; Allen, D. G. *N*-Acetylcysteine ameliorates skeletal muscle pathophysiology in mdx mice. *J. Physiol.* **586:**2003––2014; 2008.
[16] Youdim, M. B.; Edmondson, D.; Tipton, K. F. The therapeutic potential of monoamine oxidase inhibitors. *Nat. Rev. Neurosci.* **7:**295–309; 2006.
[17] Dalmaz, Y.; Peyrin, L.; Mamelle, J. C.; Tuil, D.; Gilly, R.; Cier, J. F. The pattern of urinary catecholamines and their metabolites in Duchenne myopathy, in relation to disease evolution. *J. Neural Transm.* **46:**17–34; 1979.
[18] Parker, J. M.; Mendell, J. R. Proximal myopathy induced by 5-HT-imipramine simulates Duchenne dystrophy. *Nature* **247:**103–104; 1974.
[19] Maurel, A.; Hernandez, C.; Kunduzova, O.; Bompart, G.; Cambon, C.; Parini, A.; Frances, B. Age-dependent increase in hydrogen peroxide production by cardiac monoamine oxidase A in rats. *Am. J. Physiol. Heart Circ. Physiol* **284:**H1460–H1467; 2003.
[20] Bianchi, P.; Kunduzova, O.; Masini, E.; Cambon, C.; Bani, D.; Raimondi, L.; Seguelas, M. H.; Nistri, S.; Colucci, W.; Leducq, N.; Parini, A. Oxidative stress by monoamine oxidase mediates receptor-independent cardiomyocyte apoptosis by serotonin and postischemic myocardial injury. *Circulation* **112:**3297–3305; 2005.
[21] Villeneuve, C.; Guilbeau-Frugier, C.; Sicard, P.; Lairez, O.; Ordener, C.; Duparc, T.; De Paulis, D.; Couderc, B.; Spreux-Varoquaux, O.; Tortosa, F.; Garnier, A.; Knauf, C.; Valet, P.; Borchi, E.; Nediani, C.; Gharib, A.; Ovize, M.; Delisle, M. B.; Parini, A.; Mialet-Perez, J. p53-PGC-1alpha pathway mediates oxidative mitochondrial damage and cardiomyocyte necrosis induced by monoamine oxidase-A upregulation: role in chronic left ventricular dysfunction in mice. *Antioxid. Redox Signal.* **18:**5–18; 2013.
[22] Manoli, I.; Le, H.; Alesci, S.; McFann, K. K.; Su, Y. A.; Kino, T.; Chrousos, G. P.; Blackman, M. R. Monoamine oxidase-A is a major target gene for glucocorticoids in human skeletal muscle cells. *FASEB J.* **19:**1359–1361; 2005.
[23] Shih, J. C.; Wu, J. B.; Chen, K. Transcriptional regulation and multiple functions of MAO genes. *J. Neural Transm.* **118:**979–986; 2011.
[24] Pepe, G.; Bertini, E.; Bonaldo, P.; Bushby, K.; Giusti, B.; de Visser, M.; Guicheney, P.; Lattanzi, G.; Merlini, L.; Muntoni, F.; Nishino, I.; Nonaka, I.; Yaou, R. B.; Sabatelli, P.; Sewry, C.; Topaloglu, H.; van der Kooi, A. Bethlem myopathy (BETHLEM) and Ullrich scleroatonic muscular dystrophy: 100th ENMC international workshop, 23–24 November 2001, Naarden, The Netherlands. *Neuromuscul. Disord.* **12:**984–993; 2002.
[25] Zhang, R. Z.; Sabatelli, P.; Pan, T. C.; Squarzoni, S.; Mattioli, E.; Bertini, E.; Pepe, G.; Chu, M. L. Effects on collagen VI mRNA stability and microfibrillar assembly of three COL6A2 mutations in two families with Ullrich congenital muscular dystrophy. *J. Biol. Chem.* **277:**43557–43564; 2002.
[26] Lampe, A. K.; Dunn, D. M.; von Niederhausern, A. C.; Hamil, C.; Aoyagi, A.; Laval, S. H.; Marie, S. K.; Chu, M. L.; Swoboda, K.; Muntoni, F.; Bonnemann, C. G.; Flanigan, K. M.; Bushby, K. M.; Weiss, R. B. Automated genomic sequence analysis of the three collagen VI genes: applications to Ullrich congenital muscular dystrophy and Bethlem myopathy. *J. Med. Genet.* **42:**108–120; 2005.
[27] Angelin, A.; Tiepolo, T.; Sabatelli, P.; Grumati, P.; Bergamin, N.; Golfieri, C.; Mattioli, E.; Gualandi, F.; Ferlini, A.; Merlini, L.; Maraldi, N. M.; Bonaldo, P.; Bernardi, P. Mitochondrial dysfunction in the pathogenesis of Ullrich congenital muscular dystrophy and prospective therapy with cyclosporins. *Proc. Natl. Acad. Sci. USA* **104:**991–996; 2007.
[28] Martoni, E.; Urciuolo, A.; Sabatelli, P.; Fabris, M.; Bovolenta, M.; Neri, M.; Grumati, P.; D'Amico, A.; Pane, M.; Mercuri, E.; Bertini, E.; Merlini, L.; Bonaldo, P.; Ferlini, A.; Gualandi, F. Identification and characterization of novel collagen VI non-canonical splicing mutations causing Ullrich congenital muscular dystrophy. *Hum. Mutat.* **30:**E662–E672; 2009.
[29] Cenni, V.; Sabatelli, P.; Mattioli, E.; Marmiroli, S.; Capanni, C.; Ognibene, A.; Squarzoni, S.; Maraldi, N. M.; Bonne, G.; Columbaro, M.; Merlini, L.; Lattanzi, G.; Lamin, A. N-terminal phosphorylation is associated with myoblast activation: impairment in Emery-Dreifuss muscular dystrophy. *J. Med. Genet.* **42:**214–220; 2005.
[30] Pfaffl, M. W. A new mathematical model for relative quantification in real-time RT-PCR. *Nucleic Acids Res.* **29:**e45; 2001.
[31] Pfaffl, M. W.; Horgan, G. W.; Dempfle, L. Relative expression software tool (REST) for group-wise comparison and statistical analysis of relative expression results in real-time PCR. *Nucleic Acids Res.* **30:**e36; 2002.
[32] Nicolli, A.; Basso, E.; Petronilli, V.; Wenger, R. M.; Bernardi, P. Interactions of cyclophilin with the mitochondrial inner membrane and regulation of the permeability transition pore, and cyclosporin A-sensitive channel. *J. Biol. Chem.* **271:**2185–2192; 1996.
[33] Billett, E. Monoamine oxidase (MAO) in human peripheral tissues. *NeuroToxicology* **25:**139–148; 2004.
[34] Merlini, L.; Angelin, A.; Tiepolo, T.; Braghetta, P.; Sabatelli, P.; Zamparelli, A.; Ferlini, A.; Maraldi, N. M.; Bonaldo, P.; Bernardi, P. Cyclosporin A corrects mitochondrial dysfunction and muscle apoptosis in patients with collagen VI myopathies. *Proc. Natl. Acad. Sci. USA* **105:**5225–5229; 2008.
[35] Canton, M.; Caffieri, S.; Dall'Acqua, F.; Di Lisa, F. PUVA-induced apoptosis involves mitochondrial dysfunction caused by the opening of the permeability transition pore. *FEBS Lett.* **522:**168–172; 2002.
[36] Angelin, A.; Bonaldo, P.; Bernardi, P. Altered threshold of the mitochondrial permeability transition pore in Ullrich congenital muscular dystrophy. *Biochim. Biophys. Acta* **1777:**893–896; 2008.
[37] Anderson, E. J.; Efird, J. T.; Davies, S. W.; O'Neal, W. T.; Darden, T. M.; Thayne, K. A.; Katunga, L. A.; Kindell, L. C.; Ferguson, T. B.; Anderson, C. A.; Chitwood, W. R.; Koutlas, T. C.; Williams, J. M.; Rodriguez, E.; Kypson, A. P. Monoamine oxidase is a major determinant of redox balance in human atrial myocardium and is associated with postoperative atrial fibrillation. *J. Am. Heart Assoc.* **3:**e000713; 2014.
[38] Gordon, P.; Dowben, R. M. Catecholamine distribution in mice afflicted with muscular dystrophy. *Am. J. Physiol.* **210:**728–732; 1966.
[39] Wright, T. L.; O'Neill, J. A.; Olson, W. H. Abnormal intrafibrillar monoamines in sex-linked muscular dystrophy. *Neurology* **23:**510–517; 1973.
[40] Kaludercic, N.; Carpi, A.; Nagayama, T.; Sivakumaran, V.; Zhu, G.; Lai, E. W.; Bedja, D.; De Mario, A.; Chen, K.; Gabrielson, K. L.; Lindsey, M. L.; Pacak, K.; Takimoto, E.; Shih, J. C.; Kass, D. A.; Di Lisa, F.; Paolocci, N. Monoamine oxidase B prompts mitochondrial and cardiac dysfunction in pressure overloaded hearts. *Antioxid. Redox Signal.* **20:**267–280; 2014.
[41] Chouchani, E. T.; Methner, C.; Nadtochiy, S. M.; Logan, A.; Pell, V. R.; Ding, S.; James, A. M.; Cocheme, H. M.; Reinhold, J.; Lilley, K. S.; Partridge, L.; Fearnley, I. M.; Robinson, A. J.; Hartley, R. C.; Smith, R. A.; Krieg, T.; Brookes, P. S.; Murphy, M. P. Cardioprotection by S-nitrosation of a cysteine switch on mitochondrial complex I. *Nat. Med* **19:**753–759; 2013.
[42] Nguyen, T. T.; Stevens, M. V.; Kohr, M.; Steenbergen, C.; Sack, M. N.; Murphy, E. Cysteine 203 of cyclophilin D is critical for cyclophilin D activation of the mitochondrial permeability transition pore. *J. Biol. Chem.* **286:**40184–40192; 2011.
[43] Wang, S. B.; Murray, C. I.; Chung, H. S.; Van Eyk, J. E. Redox regulation of mitochondrial ATP synthase. *Trends Cardiovasc. Med* **23:**14–18; 2013.
[44] Giorgio, V.; von Stockum, S.; Antoniel, M.; Fabbro, A.; Fogolari, F.; Forte, M.; Glick, G. D.; Petronilli, V.; Zoratti, M.; Szabo, I.; Lippe, G.; Bernardi, P. Dimers of mitochondrial ATP synthase form the permeability transition pore. *Proc. Natl. Acad. Sci. USA* **110:**5887–5892; 2013.
[45] Basso, E.; Fante, L.; Fowlkes, J.; Petronilli, V.; Forte, M. A.; Bernardi, P. Properties of the permeability transition pore in mitochondria devoid of cyclophilin D. *J. Biol. Chem.* **280:**18558–18561; 2005.
[46] Elrod, J. W.; Wong, R.; Mishra, S.; Vagnozzi, R. J.; Sakthievel, B.; Goonasekera, S. A.; Karch, J.; Gabel, S.; Farber, J.; Force, T.; Brown, J. H.; Murphy, E.; Molkentin, J. D. Cyclophilin D controls mitochondrial pore-dependent Ca(2+) exchange, metabolic flexibility, and propensity for heart failure in mice. *J. Clin. Invest.* **120:**3680––3687; 2010.
[47] Merlini, L.; Sabatelli, P.; Armaroli, A.; Gnudi, S.; Angelin, A.; Grumati, P.; Michelini, M. E.; Franchella, A.; Gualandi, F.; Bertini, E.; Maraldi, N. M.; Ferlini, A.; Bonaldo, P.; Bernardi, P. Cyclosporine A in Ullrich congenital muscular dystrophy: long-term results. *Oxid. Med. Cell Longev* **2011:**139194; 2011.
[48] Tidball, J. G.; Wehling-Henricks, M. The role of free radicals in the pathophysiology of muscular dystrophy. *J. Appl. Physiol.* **102:**1677–1686; 2007.
[49] Halliwell, B.; Gutteridge, J. M. The definition and measurement of antioxidants in biological systems. *Free Radic. Biol. Med.* **18:**125–126; 1995.
[50] Sabatelli, P.; Palma, E.; Angelin, A.; Squarzoni, S.; Urciuolo, A.; Pellegrini, C.; Tiepolo, T.; Bonaldo, P.; Gualandi, F.; Merlini, L.; Bernardi, P.; Maraldi, N. M. Critical evaluation of the use of cell cultures for inclusion in clinical trials of patients affected by collagen VI myopathies. *J. Cell Physiol.* **227:**2927–2935; 2012.